Structural analysis of calcium phosphate coatings produced by pulsed laser deposition at different water-vapour pressures

J. L. ARIAS, M. B. MAYOR, F. J. GARCÍA-SANZ, J. POU, B. LEÓN*, M. PÉREZ-AMOR
Departamento de Física Aplicada, Universidade de Vigo, Lagoas-Marcosende, 11, 36200 Vigo, Spain

J. C. KNOWLES†
IRC in Biomedical Materials, Queen Mary and Westfield College, Mile End Campus, London E14NS UK

Calcium phosphate coatings have been produced by pulsed laser deposition (PLD) at different water-vapour pressures. Rietveld refinement of X-ray diffraction (XRD) data allows us to determine that the structure of these coatings is apatitic with carbonate substitution for phosphate. The carbonate substitution decreases when the chamber pressure is raised, a fact that has been corroborated by Fourier transform–infrared (FT–IR) spectroscopy. Carbonate concentrations between 5 and 17 wt% have been calculated for the crystalline samples. Amorphous coatings are produced at the lowest and highest pressures due to the high carbonate concentration in the first case, and possibly to another type of substitution (Mg^{2+}, HPO_4^{2-}, $P_2O_7^{4-}$) or the inherent kinetics of the PLD process, in the second case.

1. Introduction

Hydroxyapatite (HA) coatings have been studied with the objective of improving the fixation and osteointegration of cementless orthopaedic and dental implant devices [1], because their chemical composition and structure are similar to the mineral phase of the bone. HA belongs to the hexagonal system with a space group $P6_3/m$ [2], characterized by a six-fold *c*-axis perpendicular to three equivalent *a*-axes at angles of 120° to each other. The dimensions of the unit cell of HA [3] are *a*-axis = 0.9422 nm, *c*-axis = 0.6880 nm ($\pm$ 0.0003 nm). The HA structure allows the substitution of many ions (K^+, Na^+, Mg^{2+}, F^-, Cl^-, CO_3^{2-}, HPO_4^{2-}, ...), which introduce changes in the unit cell dimensions.

The commercially coated biomedical implant devices are commonly produced by plasma spraying, a technique presenting problems caused by the degradation of the coating and the poor mechanical bond strength between the coating and the substrate. In an attempt to obtain properties suitable for biomedical applications, pulsed laser deposition (PLD) has been developed as a coating technique for HA [4–6]. In this work, the crystal structure of the coatings produced by PLD was studied, when the water-vapour pressure in the deposition chamber was changed.

2. Materials and methods

2.1. HA targets

Sintered HA discs were used as targets to produce the calcium phosphate coatings by pulsed laser deposition (PLD). The raw powder was uniaxially pressed at 81 MPa in a stainless steel die to form discs, and then sintered in air at 1260 °C for 4 h using heating and cooling rates of 2.5 °C min^{-1} in order to obtain targets with a density of at least 95% of the theoretical density of HA. The X-ray diffraction (XRD) and Fourier transform–infrared spectroscopy (FT–IR) analyses of the obtained targets were typical of HA with some carbonate (CO_3^{2-}) substitution for phosphate (PO_4^{3-}) and low content of hydroxyl (OH^-) groups. X-ray flourescence (XRF) measurements of the powder determined that its calcium to phosphorus ratio was 1.70, and it presented traces of magnesium (0.27 wt %).

2.2. Pulsed laser deposition (PLD)

In the PLD technique, the laser beam of a Lambda Physik LPX200 ArF excimer laser (wavelength $\lambda = 193$ nm, 20 ns pulse length, 20 Hz repetition rate) was focused on to a sintered HA disc, placed in a vacuum chamber filled with water-vapour, to achieve an

* Author to whom all correspondence should be addressed.
† *Present adress*: Department of Biomaterials, Eastman Dental Institute, 256 Gray's Inn Road, London WC1 8LD, UK
Selected paper from the 13th European Conference on Biomaterials, Göteborg, Sweden.

energy density of 0.8 J cm^{-2}. The material ablated from the HA disc was deposited on to a titanium substrate, positioned parallel to the target at 4.5 cm from it, and maintained at 455 °C at different water-vapour pressures, obtaining coatings with a thickness of 0.83 μm, as measured with a Veeco Dektak^3 profilometer.

2.3. X-ray diffraction analysis (XRD)

XRD analysis of the coatings on titanium substrates was carried out with a Siemens D-5000 diffractometer in θ–2θ configuration, using CuK_α radiation at 40 kV and 30 mA. The coatings were scanned from 10°–60° in steps of 0.02° 2θ for 15 s, and rotated during the measurement. These XRD spectra were compared with the Joint Committee of Powder Diffraction Standard (JCPDS) files. The crystal structure of the crystalline coatings was refined by the Rietveld method, using the General Structure Analysis System (GSAS) software [7].

2.4. Infrared spectroscopic analysis

Absorbance infrared spectra of the coatings on titanium substrates were collected with a Bomem MB-100 Fourier transform–infrared (FT–IR) spectrometer in reflectance with a spectral resolution of 4 cm^{-1}.

3. Results and discussion

The XRD patterns of the coatings are shown in Fig. 1. The coatings produced at 0.15 mbar show a broad peak in the range where the main peaks of the apatitic structure are located. At 0.30 mbar the structure of the apatite is completely defined, with the (2 1 1) and (1 1 2) reflections not resolved. When the pressure is increased, the coatings become less crystalline, with the reflections disappearing at 0.80 mbar.

The refined unit-cell parameters of the crystalline coatings are presented in Table I. The *a*-axis of these coatings is shorter than that of stoichiometric HA and the *c*-axis longer. This distorsion of the unit cell can be due to several factors:

(i) Ionic substitutions in the apatite lattice. The accommodation of the lattice to receive a substituting ion leads to the change in the unit-cell dimensions.

(ii) Residual stresses in the coating. Because the coatings are very thin (0.83 μm) and are produced at high temperatures (455 °C), some residual stress can exist because of the different thermal expansion coefficients of the substrate (titanium) and the apatite coating [8].

The shortening of the *a*-axis and the simultaneous lengthening of the *c*-axis is a typical effect of carbonate substitution for phosphate in the apatite lattice [9]. This point is corroborated by the FT–IR spectra of these coatings (Fig. 2), which clearly show the carbonate bands at positions characteristic of substitution for phosphate [10]: 873 cm^{-1} (ν_2 vibrational mode), and 1413 and 1454 cm^{-1} (ν_3 mode).

When the deposition pressure is raised between 0.30 and 0.60 mbar, the *a*-axis length of the unit cell of the coatings increases, while the *c*-axis slightly decreases (Table I). Although this change in the unit-cell dimensions could be due to other factors, such as any other substitution or the presence of residual stresses in the coatings, it is commonly considered as a reduction of the carbonate substitution in the apatite lattice [9, 11, 12]. In fact, the FT–IR spectra of the crystalline coatings (Fig. 2) confirm this point, because the intensity

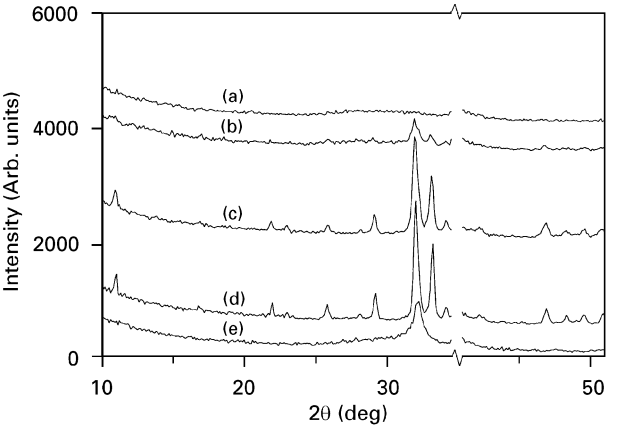

Figure 1 XRD patterns of the coatings produced by PLD at different deposition pressures of H_2O: (a) 0.80, (b) 0.60, (c) 0.45, (d) 0.30, and (e) 0.15 mbar.

TABLE I Unit-cell parameters for HA [3] and the coatings produced at different deposition pressures

Pressure (mbar)	Unit-cell parameters	
	a-axis (nm)	*c*-axis (nm)
0.30	0.9356 ± 0.0002	0.6918 ± 0.0001
0.45	0.9381 ± 0.0002	0.6910 ± 0.0001
0.60	0.9397 ± 0.0003	0.6910 ± 0.0002
Stoichiometric HA	0.9422 ± 0.0003	0.6880 ± 0.0003

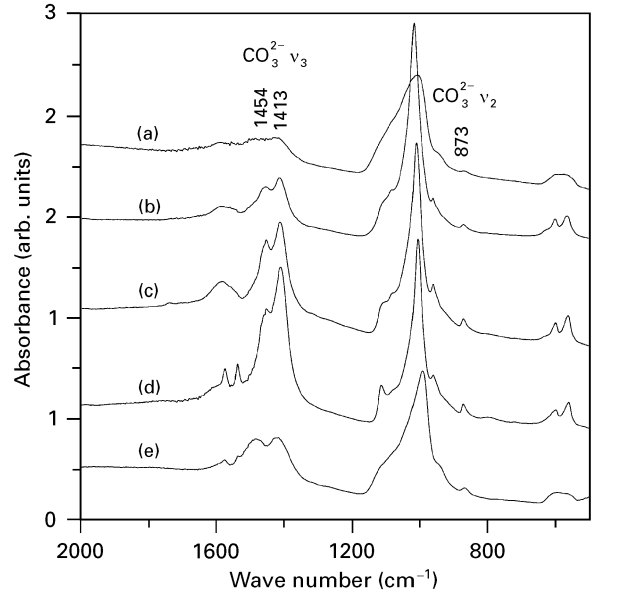

Figure 2 FT–IR spectra of the coatings produced by PLD at different deposition pressures of H_2O: (a) 0.80, (b) 0.60, (c) 0.45, (d) 0.30, and (e) 0.15 mbar.

of the ν_3 carbonate band at 1413 cm^{-1} diminishes when the deposition pressure is increased.

Arends and Davidson [13] found a linear relation between the extinction coefficient of the carbonate band at 1413 cm^{-1} and the carbonate content for different carbonated apatites. Using the molecular extinction coefficient obtained from this linear regression, the carbonate content of the crystalline coatings produced by PLD has been estimated from the extinction coefficients of the 1413 cm^{-1} band in their FT–IR spectra by the expression

$$E = E_m ct \quad (1)$$

where E is the extinction coefficient of the band, E_m the molecular extinction coefficient of carbonate, c the carbonate concentration in the coating, and t the coating thickness. The calculated carbonate contents for the crystalline coatings produced by PLD, along with the extinction coefficients of the 1413 cm^{-1} band, are summarized in Table II.

In Fig. 3, the a unit-cell parameter is represented as a function of the carbonate content in carbonated apatites produced in aqueous solution as obtained by Legeros *et al.* [9] and Nelson and Featherstone [12]. For comparison, the data obtained for the coatings produced by PLD are included. These data follow better the behaviour of the carbonated apatites produced in aqueous solution than that of the carbonated apatites produced at high temperatures, a sensible result if one considers that the processing atmosphere in PLD was water vapour and the substrate temperature was 455 °C, far below the temperature (1100–1200 °C) used for producing them [12]. Nevertheless, the c-axis deviates from this behaviour at high pressures, probably due to other possible substitutions.

TABLE II Extinction coefficients and calculated carbonate content of the crystalline coatings produced at different deposition pressures

Pressure (mbar)	E_{1413}	CO_3 content (wt %)
0.30	0.686	17.0
0.45	0.443	9.9
0.60	0.236	5.3

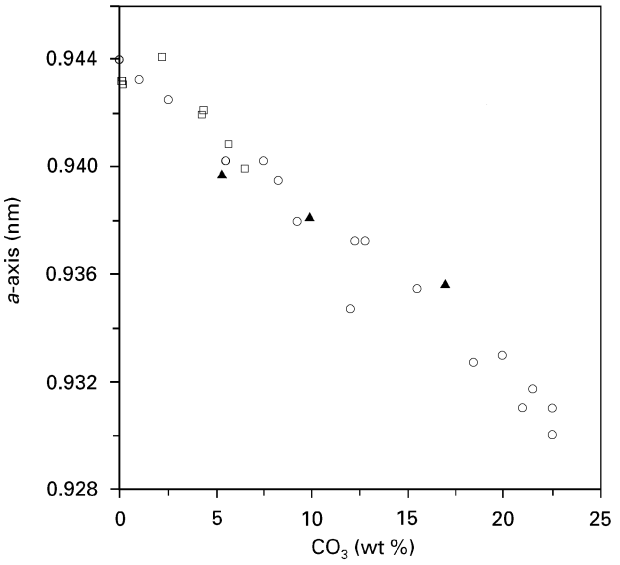

Figure 3 Unit-cell parameter a versus CO_3 content: (○) [9], (□) [12], and (▲) coatings produced by PLD.

Studies made by Legeros *et al.* [9, 14] demonstrated that the presence of carbonate in the apatite disturbs its crystallization and, at high carbonate contents, the material becomes amorphous. Therefore, the disturbance observed in the structure of the coating produced at 0.15 mbar (Fig. 1) can be explained by the high carbonate content of these coatings when the pressure is decreased.

Nevertheless, the reason for the disruption of the crystalline structure present in the coatings produced at high pressures (above 0.60 mbar) is not so clear. At these pressures, the growth rate increases and the Ca/P ratio falls below the stoichiometric HA value [15]. The following substitutions could account for the compositional change:

(a) Magnesium substitution for calcium also promotes the formation of amorphous calcium phosphates (ACP) [14], even more if combined with pyrophosphate. Traces of magnesium were found in the coatings using energy-dispersive X-ray spectroscopy analysis (EDS), but being at the detection limits it was not possible to make a comparative study between the coatings.

(b) Pyrophosphate ($P_2O_7^{4-}$) incorporation leads to ACP [14]. Although in the infrared spectra of the coatings produced at 0.30 and 0.45 mbar (Fig. 4) the pyrophosphate absorption bands at 720 and 930 cm^{-1} can be discerned, they disappear for the coatings produced at high pressures.

(c) Substitution of HPO_4^{2-} ions for phosphate introduces a high disturbance in the apatite structure [16]. These radicals give an absorption band at 864 cm^{-1}, which is too close to the ν_2 band of the carbonate ion at 873 cm^{-1} in the FT–IR spectra of these coatings to allow a more accurate analysis. A less-well resolved shoulder at 865 cm^{-1} can be observed (Fig. 4).

On the other hand, at a certain surface temperature, there is a maximum number of species having enough mobility to build up a well-structured crystalline unit cell. If the growth rate is increased by raising the deposition pressure, more species than this maximum number impinge the surface, and therefore do not have enough time to order themselves at the surface, leading possibly also to an amorphous coating, as found at 0.8 mbar.

Further experiments and other analytical techniques are being incorporated in order to assess which of these hypothesis is the correct one.

4. Conclusions

1. The crystal structure of the coatings produced by PLD is clearly dependent on the deposition pressure of water vapour.

2. A minimum pressure of water vapour is necessary to obtain a crystalline coating.

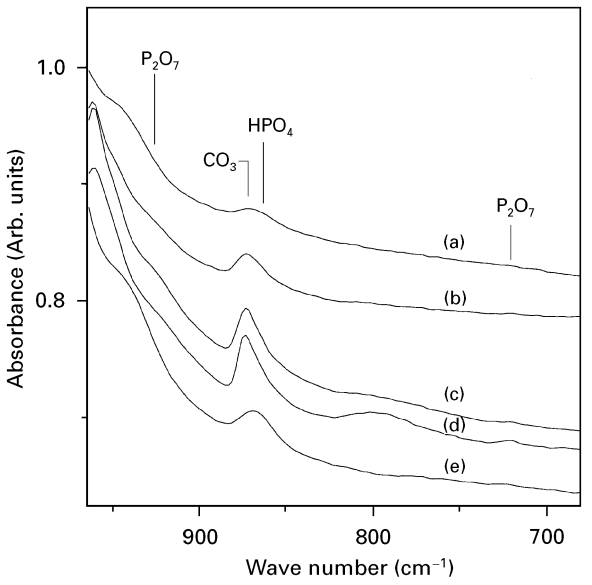

Figure 4 HPO_4^{2-}, and $P_2O_7^{4-}$ absorption bands in the FT–IR spectra of the coatings produced by PLD at different deposition pressures of H_2O: (a) 0.80, (b) 0.60, (c) 0.45, (d) 0.30, and (e) 0.15 mbar.

3. The unit-cell parameters are disturbed as a consequence of substitutions.

4. At low pressures the coatings are amorphous when the deposition pressure is decreased, due to the high carbonate content, substituting the phosphate. Comparison of the unit-cell deformation of these coatings due to the carbonate incorporation with results obtained for other techniques to produce carbonated apatites powder, indicates that PLD, although being a vacuum technique, produces material more similar to that obtained by an aqueous technology than to that achieved by a high-temperature one.

5. Coatings again become less crystalline above 0.80 mbar. Several hypotheses have been suggested, but additional work is needed to determine the ultimate reason for this last effect.

Acknowledgements

XRD analyses were performed at the C.A.C.T.I. (Universidade de Vigo). The authors aknowledge Professor W. Bonfield, IRC in Biomedical Materials, for his support and fruitful discussions. This work was partially supported by the European Union through the CRAFTcontract BRE2.CT94.1533, the Spanish government (CICYT MAT93-0271), and Xunta de Galicia (Infra 94-58).

References

1. K. DEGROOT, R. GEESINK, C. P. A. T. KLEIN and P. SEREKIAN, *J. Biomed. Mater. Res.* **21** (1987) 1375.
2. M. I. KAY, R. A. YOUNG and A. S. POSNER, *Nature* **204** (1964) 1050.
3. R. Z. LEGEROS, J. P. LEGEROS, G. DACULSI and R. KIJKOWSKA, in "Encyclopedic handbook of biomaterials and bioengineering", Part A, "Materials", Vol. 2, edited by D. L. Wise, D. J. Trantolo, D. E. Altobelli, M. J. Yaszemski, J. D. Gresser and E. R. Schwartz (Marcel Dekker, New York, 1995) pp. 1429–63.
4. C. M. COTELL, D. B. CHRISEY, K. S. GRABOWSKI and J. A. SPREGUE, *J. Appl. Biomater* **3** (1992) 87.
5. P. BAERI, L. TORRISI, N. MARINO and G. FOTI, *Appl. Surf. Sci.* **54** (1992) 210.
6. G. SARDIN, M. VARELA and J. L. MORENZA, in "Hydroxyapatite and Related Materials", edited by P. W. Brown and B. Constanz (CRC Press, Boca-Raton, 1994) pp. 225–30.
7. A. C. LARSON, R. B. VON DREELE and M. LUJAN Jr, "GSAS-General Structure Analysis System", Neutron Scattering Centre, Los Alamos National Laboratory, CA, 1990.
8. J. POU, P. GONZÁLEZ, E. GARCÍA, D. FERNÁNDEZ, J. SERRA, B. LEÓN, S. R. J. SAUNDERS and M. PÉREZ-AMOR, *Vacuum* **45** (1994) 1035.
9. R. Z. LEGEROS, O. R. TRAUTZ, J. P. LEGEROS and E. KLEIN, *Bull. Soc. Chim. Fr.* special issue (1968) 1712.
10. J. C. ELLIOT, in "International Symposium in Structural Properties of Hydroxyapatite", edited by R. A. Young and W. E. Bown (Gordon-Breach, New York, 1969).
11. C. A. BAUD and J. M. VERY, "Physico-chimie et crystallographie des apatites d'intérèt biologiques" (CNRS, Paris, 1975) pp. 101–4.
12. D. G. A. NELSON and J. B. D. FEATHERSTONE, *Calcif. Tiss. Int.* **34** (1982) S69.
13. J. ARENDS and C. L. DAVIDSON, *ibid.* **18** (1975) 65.
14. R. Z. LEGEROS, W. P. SHIRRA, M. A. MIRAVITE and J. P. LEGEROS, "Physico-chimie et crystallographie des apatites d'intérèt biologiques" (CNRS, Paris, 1975) pp. 105–15.
15. J. L. ARIAS, F. J. GARCÍA-SANZ, M. B. MAYOR, S. CHIUSSI, J. POU, B. LEÓN and M. PÉREZ-AMOR, *Biomater.* submitted.
16. G. MONTEL, "Physico-chimie et crystallographie des apatites d'intérèt biologiques", (CNRS, Paris, 1975) pp. 13–18.

Received 14 May
and accepted 15 May 1997